CONTRIBUTION ANALYSIS OF THE GRAVITY FIELD RECOVERED FROM GOCE

Weiyong Yi and Reiner Rummel

Institute of Astronomical and Physical Geodesy, Technical University Munich, Arcisstrasse 21, 80290 Munich, Germany.
Email: Weiyong.yi@bv.tum.de

Abstract

Gravity field modeling in the case of GOCE is based on a combination of the SST contribution for the low wavelength part and on gravitational gradiometry for the spatial details. The gradiomter part of the solution is derived from a combination of the gradient components V_{xx}, V_{yy}, V_{zz}. Variance components in the domain of spherical harmonics allow the analysis of the characteristic contribution of each of these groups of measurements. In the space domain, the comparison between partially combined solutions and the fully combined solution shows the functional behavior, corresponding to the error characteristics of the individual components.

Our preliminary results show that the performance of GOCE is higher than that of GRACE for the coefficients higher than about degree 145. The posteriori estimation of the variance components indicates that the performance of the gradiometer meets the requirements.

Key words: GOCE; Variance component; Satellite gradiometry; Satellite to satellite tracking.

1. Introduction

Based on the normal matrices computed separately from satellite-to-satellite tracking (SST), the three components of satellite gravitational gradiometry (SGG), as well as a constraint for the polar areas, the contributions of different data sources are computed from the resolution matrices. Since there are no measurements over the polar areas, pseudo observations are introduced at a $1^\circ \times 1^\circ$ grid at latitudes [-90° -83°] and [83° 90°]. For the contribution analysis, geoid heights of EGM08 up to degree and order 150 are introduced at the grid points with an assumed standard deviation of 10 cm, in order to compensate for the instability of the normal equation due to the polar gaps.

The normal matrix from SST is constructed based on the integral equation approach. The normal matrices from SGG are computed with the observation equations filtered into the measurement band width (MBW), i.e. [5 100] mHz.

For the contribution analysis, the gravitational model is set up to d/o 150. With the same idea, also a model up to d/o 210 is estimated. The computation is carried out with GOCE measurements from November 2009 till June 2010.

2. Methodology

We start with the combination of the normal equations from SST and SGG to determine the gravitational field

$$\left(\frac{1}{\sigma_{sst}^2}\mathbf{A}_{sst}^T\mathbf{P}_{sst}\mathbf{A}_{sst}+\frac{1}{\sigma_{sgg}^2}\mathbf{A}_{sgg}^T\mathbf{P}_{sgg}\mathbf{A}_{sgg}\right)\delta\hat{\mathbf{x}}= \left(\frac{1}{\sigma_{sst}^2}\mathbf{A}_{sst}^T\mathbf{P}_{sst}\mathbf{d}_{sst}+\frac{1}{\sigma_{sgg}^2}\mathbf{A}_{sgg}^T\mathbf{P}_{sgg}\mathbf{d}_{sgg}\right) \quad (1)$$

with the self-explanatory subscripts, $\mathbf{A}$ is design matrix computed along the orbits; $\mathbf{P}$ is the weight matrix of the observations; σ is standard deviation of unit weight (variance component); and $\mathbf{d}$ is the vector of the observed minus computed values. In order to evaluate the contribution from individual data sources, the SGG part is separated into three diagonal components (or even four if one uses the V_{xz} component too). The regularization with pseudo observations in the polar areas is also taken into account. The complete normal matrix $\mathbf{N} = \mathbf{A^T P A}$ can be written as

$$\mathbf{N}=\frac{1}{\sigma_{sst}^2}\mathbf{N}_{sst}+\frac{1}{\sigma_{xx}^2}\mathbf{N}_{xx}+\frac{1}{\sigma_{yy}^2}\mathbf{N}_{yy}+\frac{1}{\sigma_{zz}^2}\mathbf{N}_{zz}+\frac{1}{\sigma_{reg}^2}\mathbf{N}_{reg} \quad (2)$$

Thus, one obtains the *resolution matrices*:

$$\mathbf{R}_{sst} = \mathbf{N}^{-1}\frac{1}{\sigma^2_{sst}}\mathbf{N}_{sst}, \qquad \mathbf{R}_{xx} = \mathbf{N}^{-1}\frac{1}{\sigma^2_{xx}}\mathbf{N}_{xx},$$
$$\mathbf{R}_{yy} = \mathbf{N}^{-1}\frac{1}{\sigma^2_{yy}}\mathbf{N}_{yy}, \qquad \mathbf{R}_{zz} = \mathbf{N}^{-1}\frac{1}{\sigma^2_{zz}}\mathbf{N}_{zz}, \qquad (3)$$
$$\mathbf{R}_{reg} = \mathbf{N}^{-1}\frac{1}{\sigma^2_{reg}}\mathbf{N}_{reg}$$

They add up to the unit matrix, see [1]: $\mathbf{R}_{sst}+\mathbf{R}_{xx}+\mathbf{R}_{yy}+\mathbf{R}_{zz}+\mathbf{R}_{reg} = \mathbf{I}$. It can be shown that

$$E\{\delta\hat{\mathbf{x}}\} = (\mathbf{R}_{sst}+\mathbf{R}_{xx}+\mathbf{R}_{yy}+\mathbf{R}_{zz}+\mathbf{R}_{reg})\,\delta\mathbf{x} = \delta\mathbf{x} \quad (4)$$

The resolution matrices are a measure of the relative contribution from the different data sources. They behave as filters through which the vector $\delta\mathbf{x}$ passes to yield the estimator $\delta\hat{\mathbf{x}}$, see [2, 1]. One may notice that the resolution matrices are computed from only the normal matrices, without any information from the measurements or a priori values. Therefore it is an important and reliable tool to identify how much contribution one can expect from different data sources, and a priori information as well.

The main diagonal elements in the resolution matrices in Equation 3 give the contribution measure for individual parameters. For the i^{th} parameter, the contribution from the different sources are

$$r_{sst_i} = [\mathbf{R}_{sst}]_{ii}, \qquad r_{xx_i} = [\mathbf{R}_{xx}]_{ii},$$
$$r_{yy_i} = [\mathbf{R}_{yy}]_{ii}, \qquad r_{zz_i} = [\mathbf{R}_{zz}]_{ii}, \qquad (5)$$
$$r_{reg_i} = [\mathbf{R}_{reg}]_{ii}$$

The variance components are the relative weight for different data sources. The a priori estimate of the variance components for observation type j is obtained from [3]

$$\hat{\sigma}_j^{2(-)} = \frac{\mathbf{d}_j^T\mathbf{P}_j\mathbf{d}_j}{n_j} - \left(\frac{1}{n_j}\sum_{k=1}^{n} d_{j(k)}\right)^2 \qquad (6)$$

with d the observed minus computed values as in Equation 1, $\mathbf{P}$ the weight matrix, n the number of the observations.

The posteriori estimation is computed with

$$\hat{\sigma}_j^2 = \frac{\mathbf{d}_j^T\mathbf{P}_j\mathbf{d}_j - \delta\hat{\mathbf{x}}_j^T\mathbf{N}_j\delta\hat{\mathbf{x}}_j}{n_j - t_j} \qquad (7)$$

where $\delta\hat{\mathbf{x}}_j$ is the vector of estimated parameters from observation type j, and t_j is the number of parameters.

3. Contribution based on posteriori estimation of the variance components

Based on the normal equations from various components, the contribution from all the involved data types are computed. The contribution from SST is shown in Figure 1.

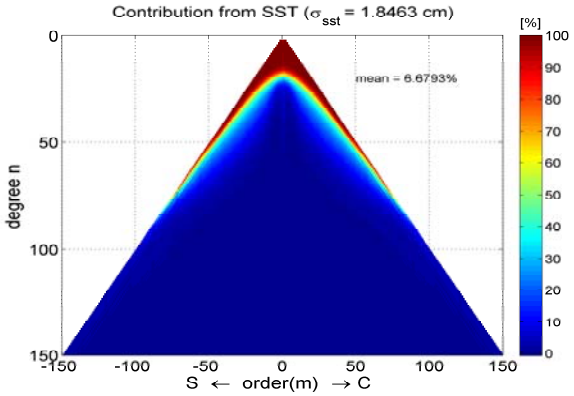

Figure 1: Contribution from SST.

From Figure 1 one can see that SST contributes mainly to the lower degrees and orders and especially to their sectorial part. The square root of the estimated posteriori variance component is 1.85 cm, which is approximately equal to the precision of the kinematic orbits, cf. [4].

The contribution from pseudo observations is presented in Figure 2. One can see is important but rather small, which means the a priori information affects the final solution only moderately.

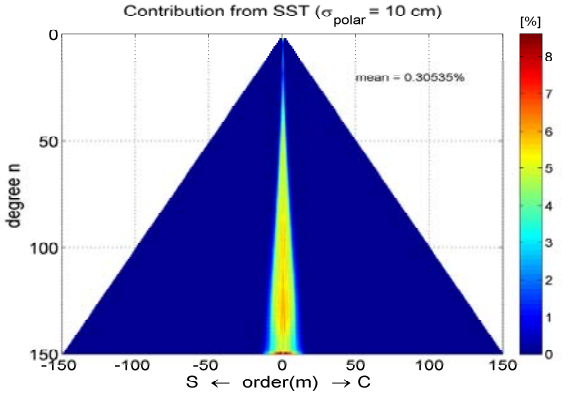

Figure 2: Contribution from pseudo observations.

As shown in Figure 3, 4 and 5, the contributions from three diagonal components are complementary for the higher degree coefficients. The V_{xx} component contributes more information to the lower order coefficients (zonals), the V_{yy} component more to the higher order coefficients (sectorials), and as to be expected - the contribution from the V_{zz} component are quite homogeneous

compared to those of V_{xx} and V_{yy}. Although the signal in V_{zz} is larger than that of the other two components, its contribution is less, due to its higher noise level in the MBW, see [5].

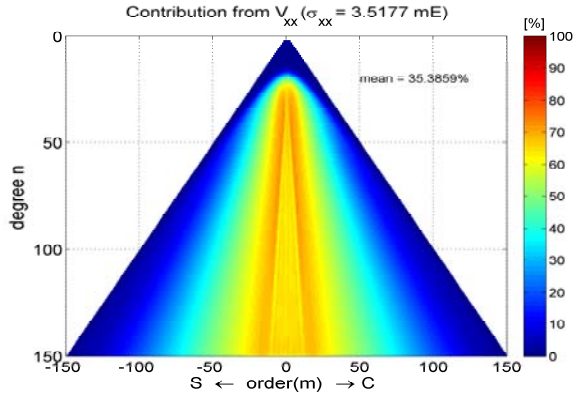

Figure 3: Contribution from V_{xx}.

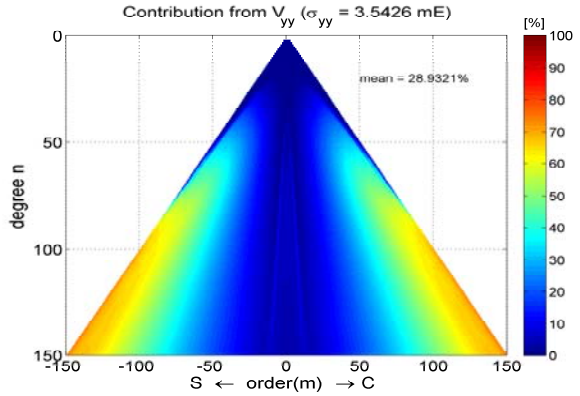

Figure 4: Contribution from V_{yy}.

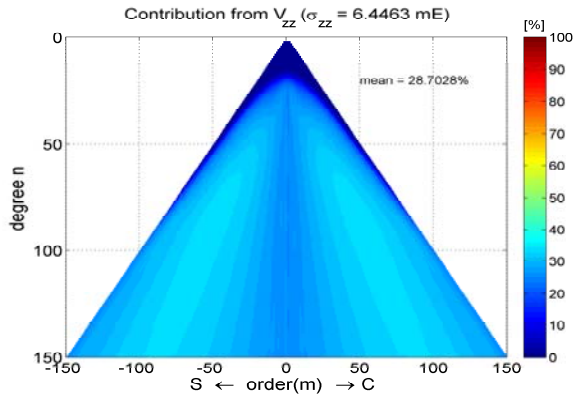

Figure 5: Contribution from V_{zz}.

The posteriori estimation of the variance components of V_{xx}, V_{yy} and V_{zz} is 3.5117 mE, 3.5426 mE and 6.4463 mE, repectively. These values can be considered as the precision of the three diagonal components, since they are computed based on the posteriori estimation, therefore without any effect from a priori information.

In Figure 6, the contribution from all the data sources considered are presented for the degrees n=19 and n=135. For lower degree coefficients, the dominant contributions come from the SST part. There is little contribution from SST to the coefficients of degree 135, the contributions from SGG are therefore dominant and complementary.

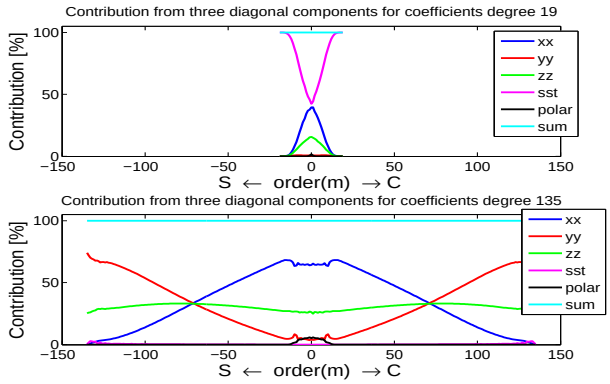

Figure 6: Contributions from different data sources for degrees 19 and 135.

4. Comparison of individual components to the fully combined solution

In order to study the contribution from different components in the space domain, the geoid differences between models recovered from SST (and pseudo obs. in polar areas) combined with each of the diagonal components of SGG, individually, to the combined solution of all observations are presented in Figures 7, 8 and 9.

The standard deviation (std) of the difference between the partially combined V_{zz} component and the fully combined solution is less than that of the other two components. This is due to the homogeneity of the V_{zz}, compare Figure 5. The large std in Figure 7 and 8 is because the precision of the coefficients estimated with these two components is uneven, as shown in Figures 3 and 4. The error behavior for the components V_{xx} and V_{yy} can be found, as shown the north-south and east-west stripes, respectively, although The measurements are collected in the Gradiometer Reference Frame (GRF), which slightly deviates from the Local Orbital Reference Frame (LORF).

The gravity anomaly map of the fully combined solution up to degree and order 150 with respect to WGS84 is shown in Figure 10. The geophysical features such as Himalaya, Andes, Mid-Atlantic ridge, etc., can be clearly seen.

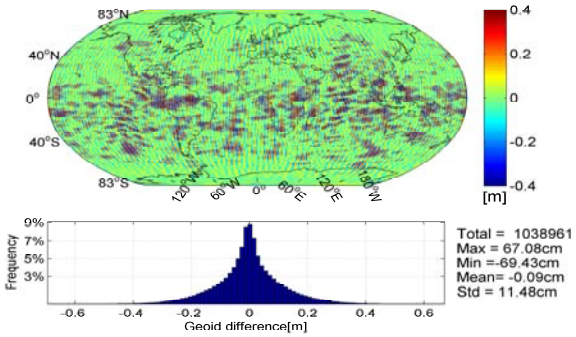

Figure 7: Geoid differences between V_{xx} (combined with SST and pseudo obs.) to the fully combined solution.

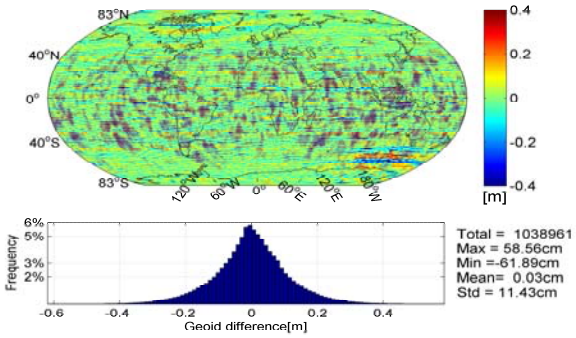

Figure 8: Geoid differences between V_{yy} (combined with SST and pseudo obs.) to the fully combined solution.

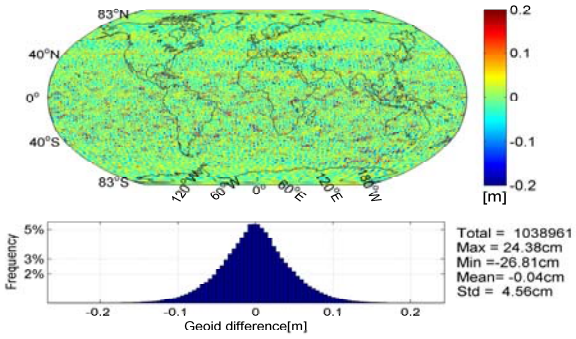

Figure 9: Geoid differences between V_{zz} (combined with SST and pseudo obs.) to the fully combined solution.

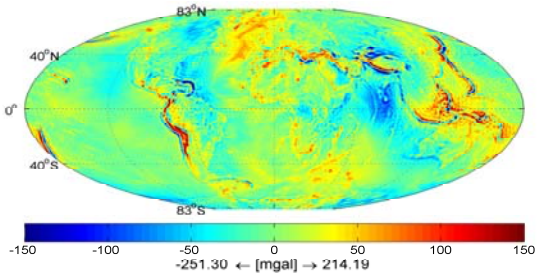

Figure 10: Gravity anomaly map of the fully combined solution relative to WGS84 (d/o 150).

5. Solution compared to independent models

Following the same approach, a model complete up to d/o 210 has been developed from the same period of data. The degree root mean square (RMS) of the fully combined solution compared to EGM2008 and ITG-Grace2010s is presented in Figure 11.

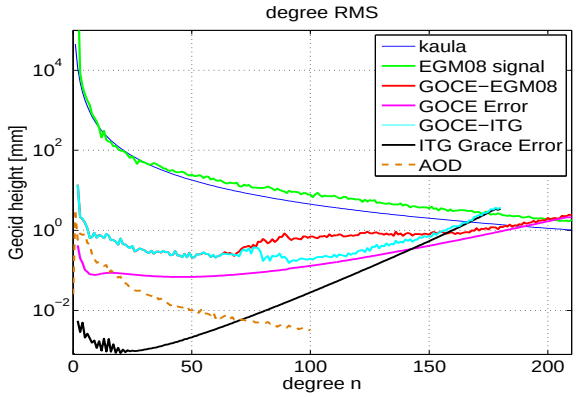

Figure 11: Degree RMS of the solution comparing to EGM2008 and ITG-Grace2010s.

From the formal error in Figure 11, one can see that GOCE gravity coefficients are better at degrees higher than 145. Both the formal error and the differences to EGM2008 reach the same magnitude of the reference signal at about degree 205. This is consistent with the analysis made in [6].

In Figure 12 the geoid difference between the fully combined solution to EGM2008 up to d/o 200 are presented. The RMS of the difference is 18 cm. Large differences are found in Himalaya, South America and Africa. The terrestial data in these areas used for EGM2008 are less accurate than in the other areas.

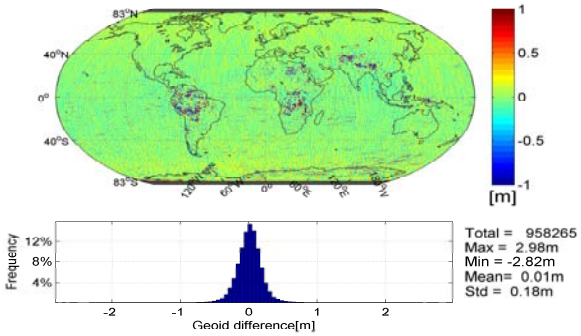

Figure 12: Geoid differences between the combined solution and EGM2008 (d/o 200).

6. Conclusions

The contributions of the GOCE gravity gradient components V_{xx}, V_{yy} and V_{zz} are complementary. Since the noise in V_{zz} is higher than the other two, its contribution is less than expected. Despite of that, the V_{zz} shows very good consistency to the fully combined solution, due to its good spatial homogeneity. This property reduces the standard deviation of geoid difference between partially combined solution of V_{zz} to the fully combined solution and makes it smaller than those of V_{xx} and V_{yy}. In this sense, one can say V_{zz} is still a very powerful component. From the analysis in the spherical harmonics, the contribution from V_{xx} is the largest, whereas V_{yy} and V_{zz} have similar magnitude of contribution. Pseudo observations in the polar areas are used to stabilize the computation and de-correlate the zonal and near zonal coefficients. They have, however, less than 1% contribution to the final result. The SST contributes more information to the lower degree coefficients and especially of the higher orders. The posteriori estimation of the orbit error is about 1.85 cm, which is less than the requirement, i.e., 2 cm. In our computation, we found the posteriori estimation of the variance components of V_{xx}, V_{yy} and V_{zz} are quite small and the square root of their squared sum is less than 11 mE, i.e., less than the requirements of the trace in the MBW. These values are the square root of unit weight error, which are very reliable and powerful quantities to indicate the performance of the whole system, including sensor and data pre-processing, parameter estimation.

About half year of GOCE data shows better performance than seven years of GRACE data at degrees higher than about 145. Large geoid differences between our solution and EGM08 can be found in areas where the quality of the terrestrial data is expected to be poor, such as Himalaya and parts of Africa and South America.

Acknowledgements

The work of the first and second author is supported by the Institute for Advanced Study of Technische Universität München. Additional support of the work of the first author comes from Institute of Geodesy and Geophysics, Chinese Academy of Sciences. Supportes from Leibniz Supercomputing Centre are highly appreciated.

References

[1] Nico Sneeuw, 2000, a semi-analytical approach to gravity field analysis from satellite observations, DGK, Reihe C, Verlag der Bayerischen Akademie der Wissenschaften, München

[2] Johannes Bouman, 1997, Quality Assessment of Geopotential Models by Means of Redundancy Decomposition, DEOS Progress Letters, 97.1, 49-54

[3] Montenbruck O, Gill E (2000) Satellite Orbits: Models, Methods and Applications, 1st edn. Springer, Berlin

[4] H. Bock , A. Jäggi , U. Meyer , G. Beutler , P. Visser , J. van den IJssel , T. van Helleputte , M. Heinze , U. Hugentobler , C. Förste, 2010, Rapid and Precise Orbit Determination for the GOCE Satellite, Presented at EGU-2010, Vienna, Austria

[5] Yi W, Murböck M, Rummel R, Gruber T, 2000, Performance Analysis of GOCE Gradiometer Mearsurements, ESA Living Planet Symposium, Bergen, Norwegen

[6] Reiner Rummel, Weiyong Yi, Claudia Stummer, 2010, GOCE gravitational gradiometry, Submitted to J Geod.